A REANALYSIS OF HIGH RESOLUTION X-RAY DATA OF V2491 CYG USING HOT/WARM ABSORBER MODELS

Şölen Balman
and
Çiğdem Gamsızkan
Middle East Technical University, Ankara, Turkey

From Cooling to Explosions : The Physics of White Dwarfs – Hernanzfest, 14-16 Jun 2017

ON THE STELLAR REMNANT EMISSION IN NOVAE

- ✓ First attempts on model spectra → blackbody models → super-Eddington luminosities for the stellar remnant (see, Ögelman+ 1993).
- ✓ To overcome the super-Eddington luminosity problem and to incorporate the abundance and ionization edge effects of C-O and O-Ne core WDs, LTE (Local Thermodynamic Equilibrium) models were used with the ROSAT and Beppo-Sax data with success (Balman+ 1998, Kahabka+ 1999, Balman & Krautter 2001).
- ✓ In the X-ray gratings Era, → detailed structure with emission and absorption features. Spectral modeling from the stellar remnants have been done using hydrostatic NLTE atmosphere models (Orio+ 2002; Nelson+ 2008; Rauch+ 2010; Osborne+ 2011; Ness+ 2011; Tofflemire+ 2013) → account for the absorption edges/lines from a static atmosphere.
- ✓ Most absorption features showed blueshifts in the spectra (e.g., Ness+ 2003, 2007) **not** modeled by the NLTE static atmospheres.
- ✓ As a solution → The stellar atmosphere code PHOENIX (Hauschildt & Baron 1999, 2004) was adjusted to model NLTE expanding atmosphere models, a hybrid atmosphere model that is hydrostatic at the base with an expanding envelope on the top. Expansion is attained by an optically thick wind from the remnant. (Petz+ 2005; van Rossum & Ness 2010). van Rossum (2012) presents a new set of expanding NLTE atmosphere models with better quality fit approximations but yet with solar composition models. → lower effective temperatures for the remnant WD in comparison with the static models (van Rossum & Ness 2010; van Rossum 2012).

V1974 CYG – ONE OF THE FIRST NOVA OBSERVED OVER THE ENTIRE ELECTROMAGNETIC SPECTRUM

- constant bolometric luminosity in the X-ray band detected for days 255-511 $F_{bol}=(1.7\text{-}2.3)\times10^{-7}$ ergs s^{-1} cm^{-2} .
- Between day 261-511 radius decreased by 26.1 ± 2.6 km/d and temp. increased by 350 ± 120 K/d. Cooling time scale in soft X-rays 300 d.

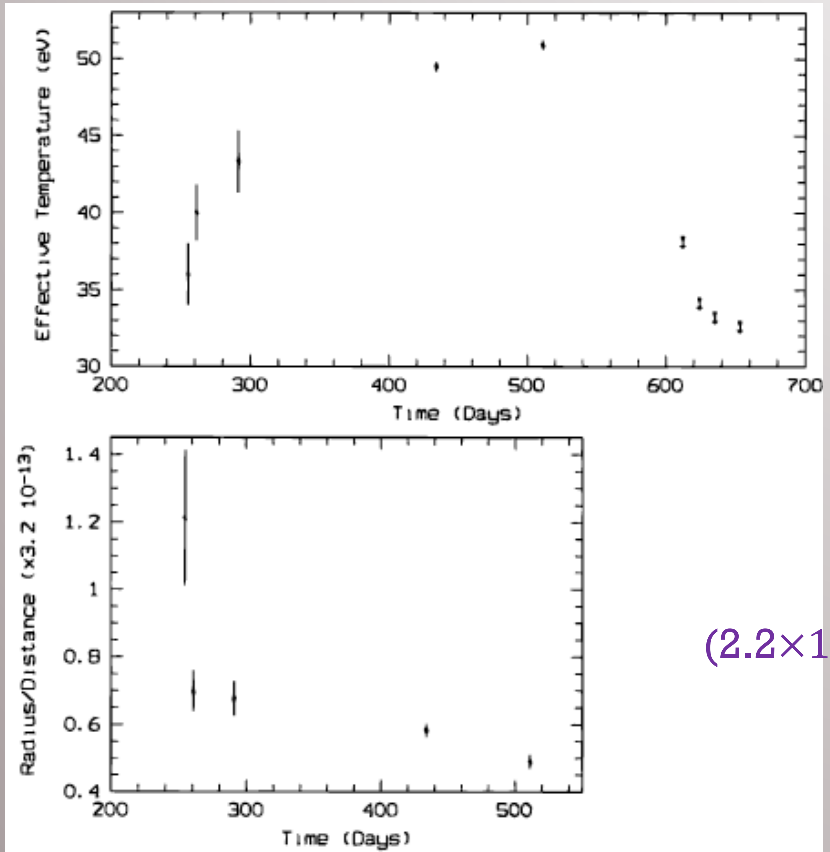

$(2.2\times10^{9} - 0.9\times10^{9})$ cm

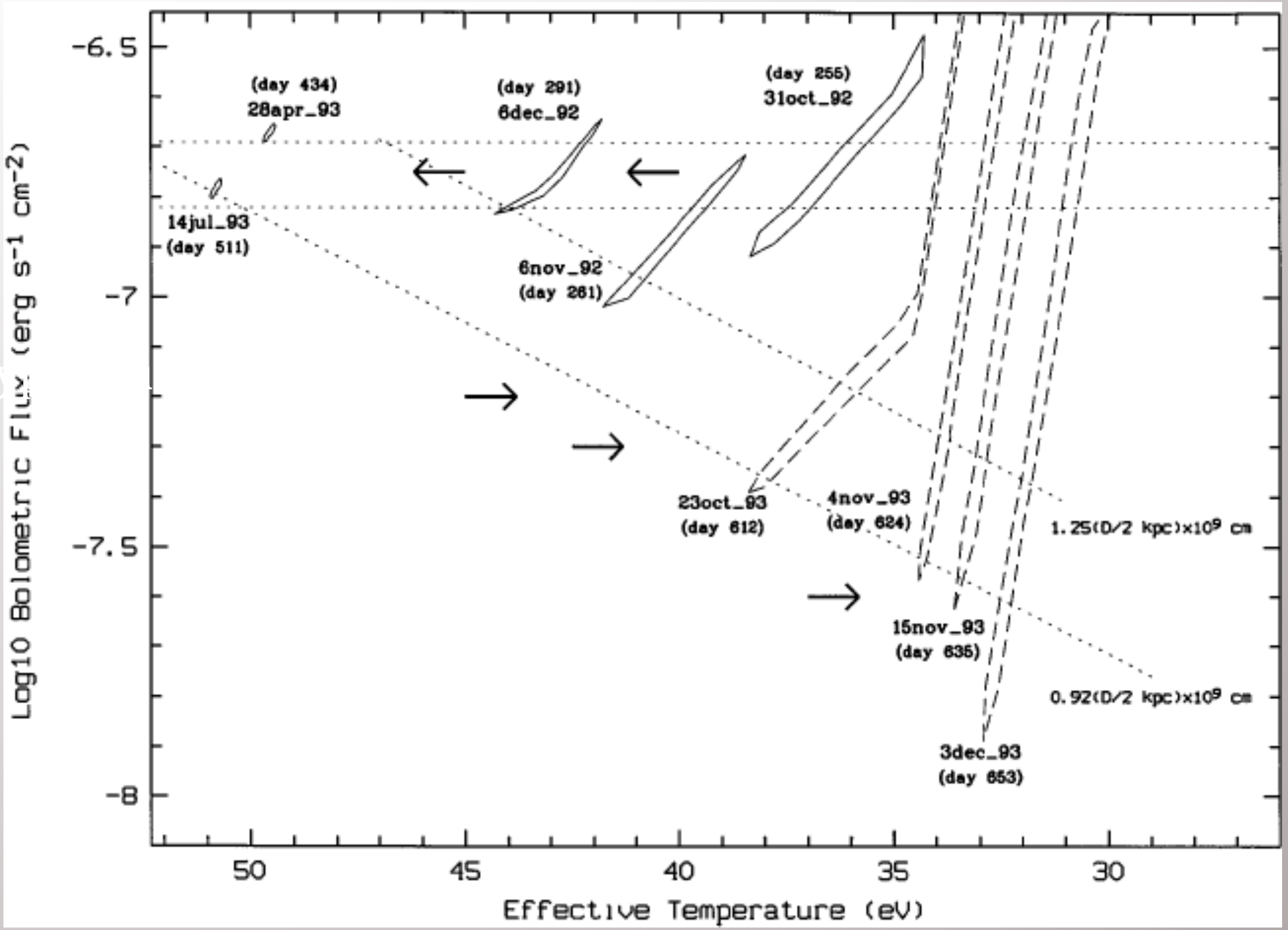

Fits with **LTE atmosphere models O-Ne** and C-O (Balman+ 1998)

V2491 CYG – NLTE ATMOSPHERE MODEL FITS

- ❖ Discovered in April 2008 (Nakano+ 2011) with $t_2 \sim$ 4.8 d
- ❖ Very fast nova like V838 Her, V2487 Oph
- ❖ He/N nova (Lynch+ 2008, Helton+ 2008)
- ❖ Very broad line structures with complex profiles and large expansion speeds (4000-6000 km/s) (Lynch+ 2008, Tomov+ 2008)
- ❖ Soft and Hard X-ray components (Page+ 2010, Ness+ 2011)
- ❖ Takei+ 2009,2011 → early nonthermal emission and reestablishment of accretion by day 50 or even by 40 d after outburst. A soft IP interpretation (38 min pulsations)+ soft BB component at 77 eV (Zemko+ 2015)
- ❖ Ness+ 2011 find blue shifts of 3000-3400 km/s and using a stellar atmosphere model that obtain temperatures 9.6-10.5×10^5 K with (2-8)×10^8 cm radius for the WD. However, the fits have χ^2_ν = 2.2-21.8 for 5600 (dof).

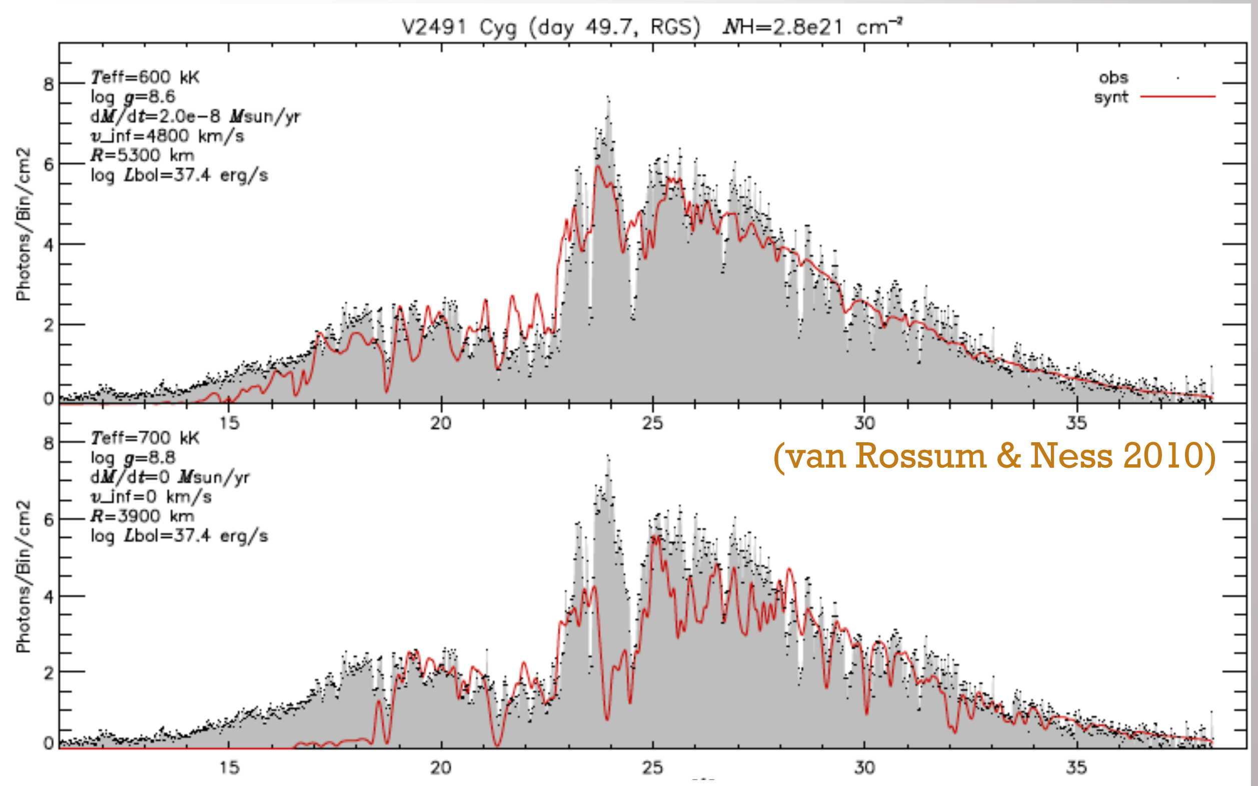

(van Rossum & Ness 2010)

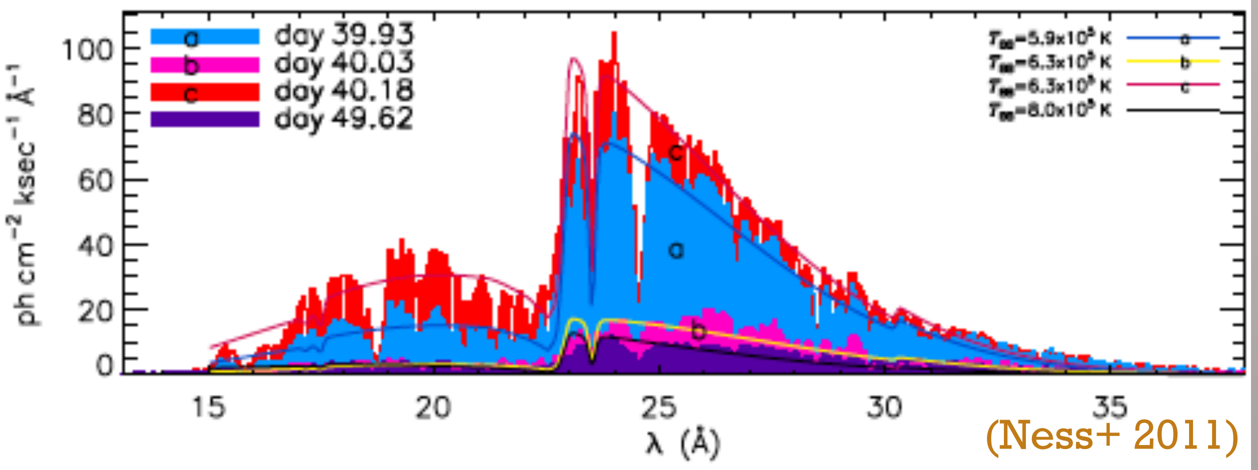

(Ness+ 2011)

MODELING VIA INTRINSIC PHOTOIONIZED ABSORPTION

Component	Parameter	A.1	A.2	A.3	B
Blackbody	R (10^7 m)	2.1 ± 0.2	1.0 ± 0.1	1.76 ± 0.03	0.19 ± 0.05
	kT_{eff} (eV)	91 ± 1	81 ± 1	121 ± 2	95 ± 1
	L_{RGS} (10^{32} W)	2.20	0.23	5.70	0.03
	L_{BOL} (10^{32} W)	4.39	0.57	8.49	0.04
CIE	$n_e n_H V$ (10^{63} m^{-3})	5.6 ± 0.7	7.1 ± 0.7	9.6 ± 0.4	5.2 ± 0.4
	kT (keV)^a	0.39 ± 0.05	0.39 ± 0.05	0.37 ± 0.05	0.71 ± 0.05
	L_{RGS} (10^{28} W)	0.79	1.05	1.40	0.94
	L_{BOL} (10^{28} W)	1.24	1.65	2.24	1.45
	σ_C (km s^{-1})	≡3000	≡3000	3000 ± 300	≡3000
	Mg/Ne	≡1.2	≡1.2	1.2 ± 0.2	≡1.2
	$\Delta\chi^2$/d.o.f.	85/2	136/2	709/4	255/2
Abundances in the shell	C/O	≡0.13	≡0.13	0.13 ± 0.01	≡0.13
	N/O	≡2.41	≡2.41	2.41 ± 0.01	≡2.41
	Si/O	≡0.015	≡0.015	0.015 ± 0.005	≡0.015
	S/O	≡0.11	≡0.11	0.11 ± 0.01	≡0.11
	Ar/O	≡0.20	≡0.20	0.20 ± 0.01	≡0.20
	Ca/O^b	≡0.01	≡0.01	≲0.01	≡0.01
	Fe/O	≡0.47	≡0.47	0.47 ± 0.01	≡0.47
Layer 1	H Col. (10^{28} m^{-2})	0.73 ± 0.02	2.13 ± 0.01	0.48 ± 0.01	1.22 ± 0.07
	O Col. (10^{25} m^{-2})	0.44 ± 0.01	1.29 ± 0.01	0.29 ± 0.01	0.74 ± 0.04
	Log ξ (10^{-9} Wm)	≳5.0	4.25 ± 0.02	≳4.9	4.38 ± 0.06
	σ_V (km s^{-1})	1230 ± 20	225 ± 35	1470 ± 10	55 ± 20
	v (km s^{-1})	−3730 ± 30	−3360 ± 70	−3620 ± 20	−4560 ± 130
	$\Delta\chi^2$/d.o.f.	526/4	609/4	4083/11	449/4
Layer 2	H Col. (10^{28} m^{-2})	2.0 ± 0.2	0.1 ± 0.05	4.15 ± 0.02	0.013 ± 0.002
	O Col. (10^{25} m^{-2})	1.2 ± 0.1	0.06 ± 0.03	2.51 ± 0.01	0.008 ± 0.001
	Log ξ (10^{-9} Wm)	3.61 ± 0.01	2.50 ± 0.05	3.76 ± 0.01	2.18 ± 0.03
	σ_V (km s^{-1})	10 ± 5	10 ± 5	20 ± 5	160 ± 10
	v (km s^{-1})	−2790 ± 20	−3260 ± 20	−2810 ± 10	−3080 ± 40
	$\Delta\chi^2$/d.o.f.	526/4	62/4	2951/11	373/4
Layer 3	H Col. (10^{25} m^{-2})	8.1 ± 0.2	0.5 ± 0.1	8.1 ± 0.2	2.6 ± 0.2
	O Col. (10^{22} m^{-2})	4.9 ± 0.1	0.30 ± 0.06	4.9 ± 0.1	1.6 ± 0.1
	Log ξ (10^{-9} Wm)	1.40 ± 0.05	≲0.01	1.36 ± 0.01	1.18 ± 0.05
	σ_V (km s^{-1})	235 ± 10	70 ± 20	200 ± 10	180 ± 20
	v (km s^{-1})	−3400 ± 30	≳−3040	−3340 ± 20	−3300 ± 50
	$\Delta\chi^2$/d.o.f.	448/4	25/4	781/11	399/4
Cold gas	Col. (10^{25} m^{-2})	2.85 ± 0.01	2.81 ± 0.01	2.24 ± 0.01	1.97 ± 0.02
	kT (eV)	1.13 ± 0.01	1.21 ± 0.01	1.04 ± 0.01	0.99 ± 0.02
	N/H	≡2.14	≡2.14	2.14 ± 0.02	≡2.14
	O/H	≡2.71	≡2.71	2.71 ± 0.01	≡2.71
	Fe/H	≡1.19	≡1.19	1.19 ± 0.03	≡1.19
Dust	O I (10^{21} m^{-2})	3.8 ± 0.1	6.3 ± 0.1	3.2 ± 0.1	5.3 ± 0.2
	$\Delta\chi^2$/d.o.f.	497/1	356/1	1300/1	948/1
Statistics	χ^2/d.o.f.	3538/1474	3980/1474	10380/1462	3390/1474

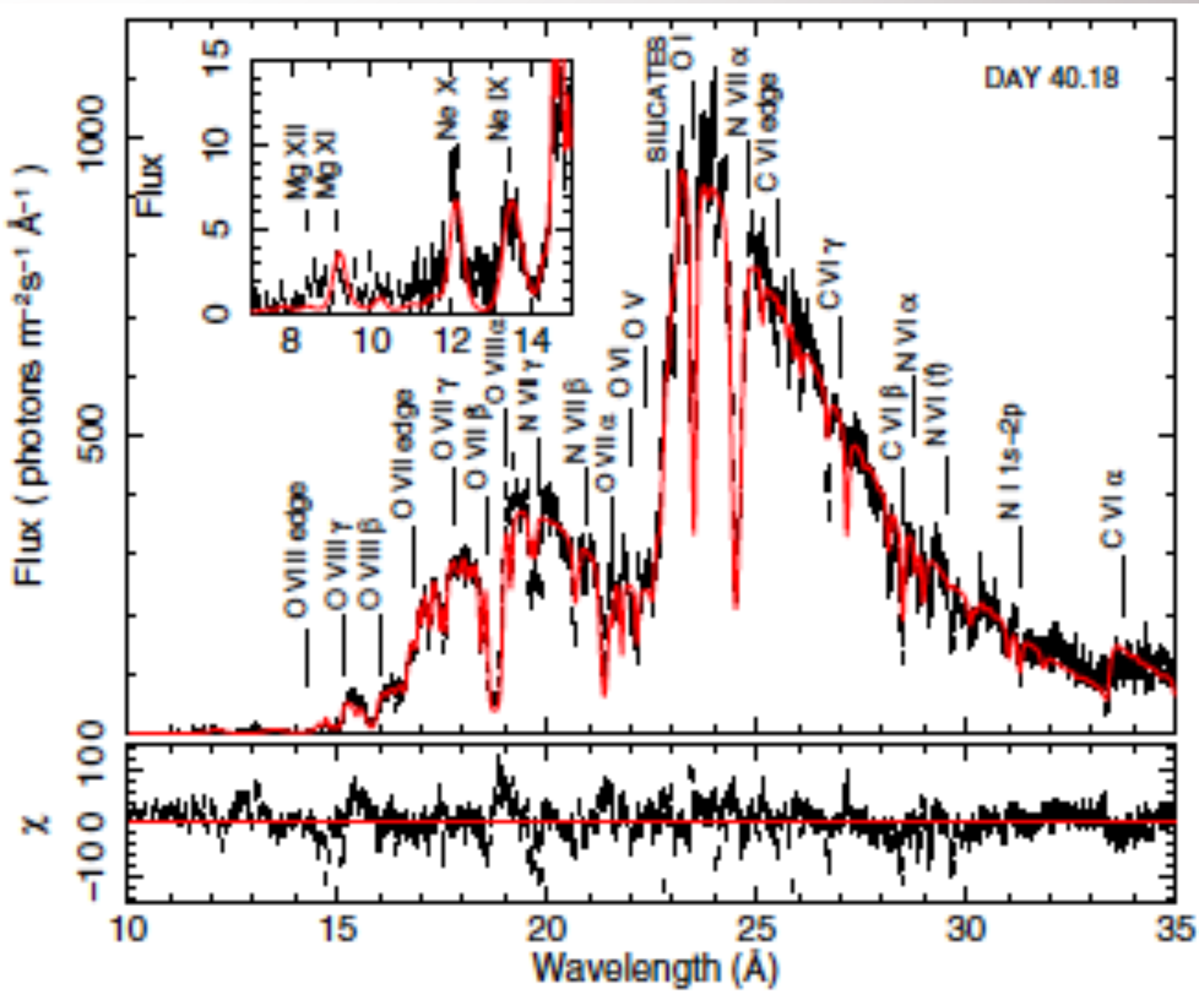

χ^2_ν = 2.3-7.0

(Pinto+ 2012)

OBSERVATIONS OF V2491 CYG -- LIGHT CURVES

Our aim is to model absorption components in the high resolution spectra independently from the continuum model. The complex absorption model → **hot collisionally ionized (in equilibrium) absorber** and photoionized warm absorber models along with interstellar absorption (of gas and dust origin separately). For continuum and line emission blackbody and plasma models are used
(see Balman & Gamsızkan 2017)

May 20, 2008 – 32 ks and May 30, 3008 29.8 ks (RGS standard spectroscopy mode)
40 and 50 days after outburst.
Three different count rate time intervals have been chosen in accordance with Pinto+ 2012

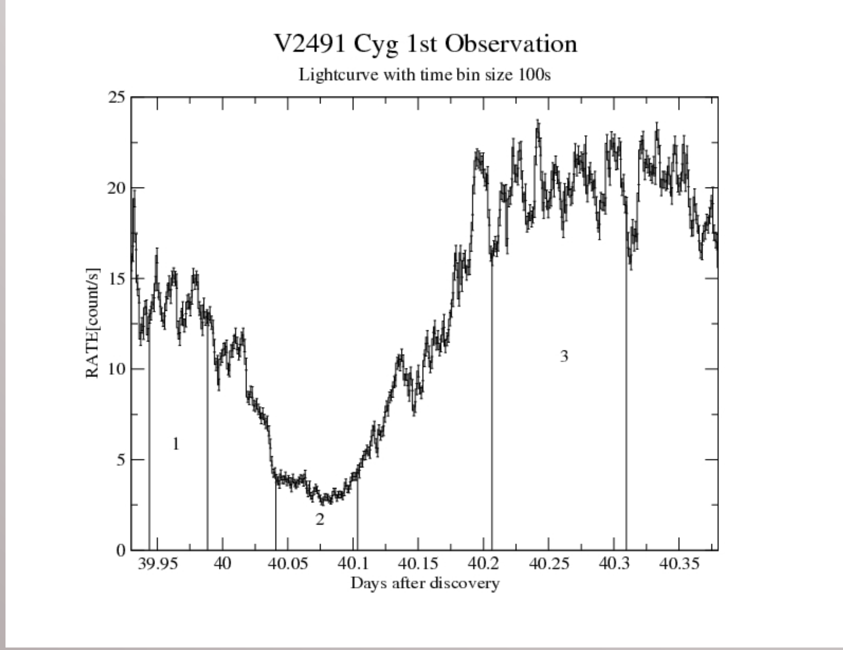

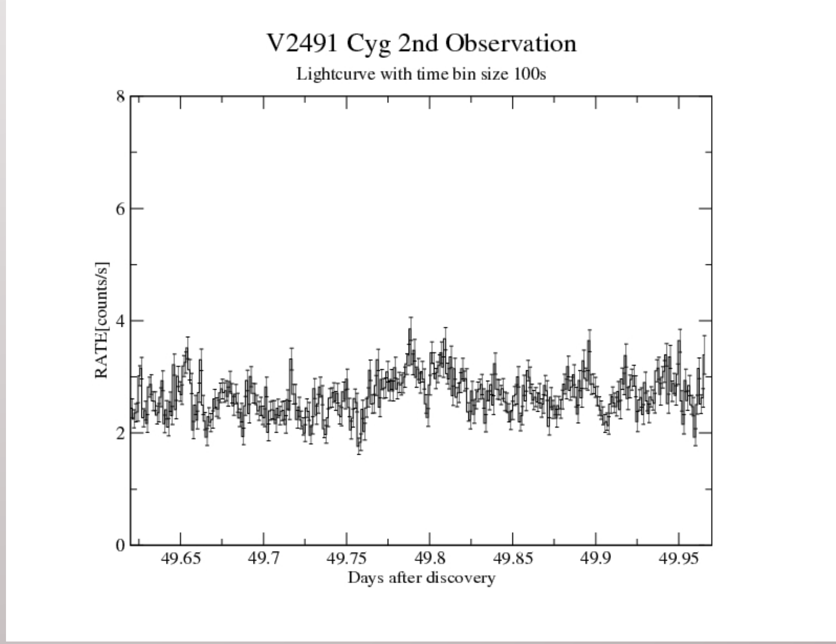

WARM ABSORBERS AND HOT ABSORBERS

- **XABS** – **Photoionized absorber model** (composed of different ions located between the ionizing source and the observer)
- Tramsmission of slab of material depends on : continuum and line absorption by the ions and (free) electron scattering out of line-of-sight (Thomson approx. < 10 keV)
- Continuum opacities (Verner & Yakovlev 1995) ; Line opacities (Verner+ 1996); abundances calculated using Lodders & Palme 2009).
- $\xi = \frac{L}{n\,r^2}$ is the ionization parameter in erg cm s^{-1}
- Broadband ionizing continuum is assumed to pre-calculate the ionic column densities for different ξ from **CLOUDY** (Ferland 2003) or XSTAR (Kallman & Bautista 2001) .

- **SPEX** (**SRON** Kaastra+1996)
- **HOT** – **Collisionally ionized absorber** model (transmission of a plasma in collisional equilibrium with cosmic abundances)
- Tramsmission of slab of material depends on : continuum and line absorption by the ions and (free) electron scattering.
- Continuum opacities (Verner & Yakovlev 1995) ; Line opacities (Verner+ 1996); abundances calculated using Lodders & Palme 2009). Mimics neutral plasma transmission around 0.5-1 eV -- gas component of ISM.
- For a given T and abundances calculates ionization balance and then determines all ionic column densities scaling from H column density and multiplying contribution of individual ions.

THE MODELLING

Harder X-ray band data (7-14.4 Å) was fitted with the **Cie** (plasma in collisional equilibrium) model together with the **cold Hot** (**Hot-ISM**) absorber model for the gas in the interstellar medium.

Detection of the second Blackbody component in the **second observation** with a temperature of **120-131 eV** and an emitting radius of **(1.3-1.8)**$\times$**10^7 cm** about **10% of the WD radius** improves the fits to acceptable χ^2_ν Levels with improving global fits at 93%-95% Confidence Levels.

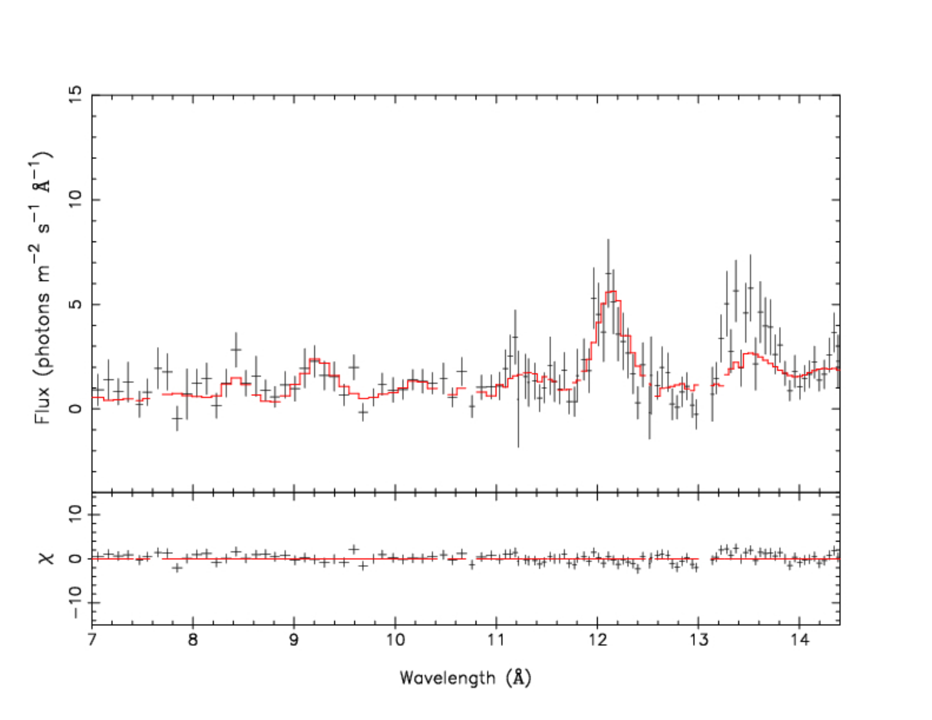

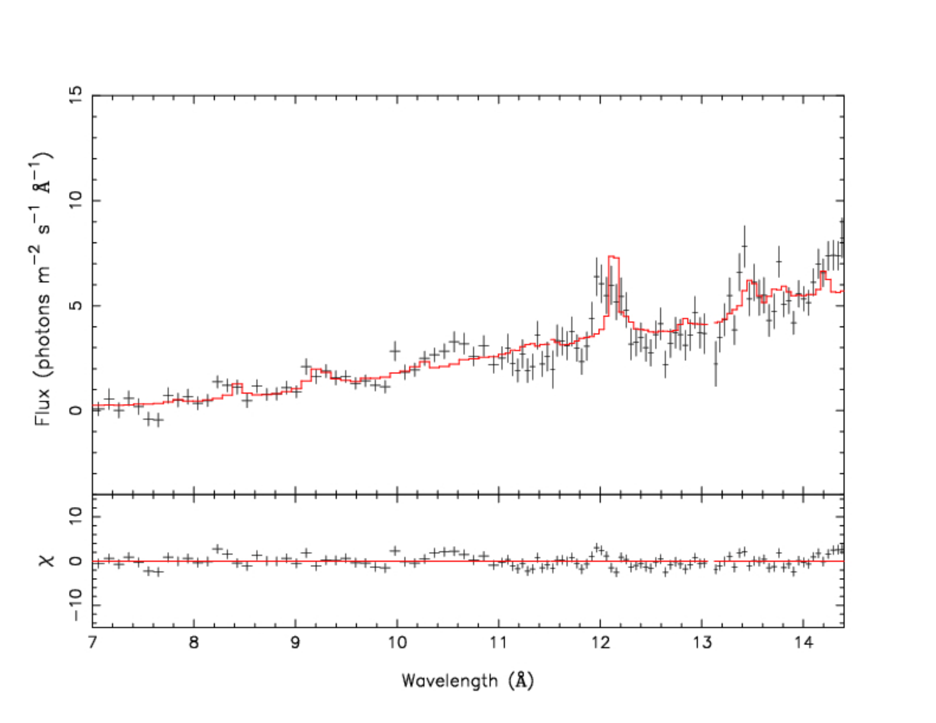

Region 1 (A1)

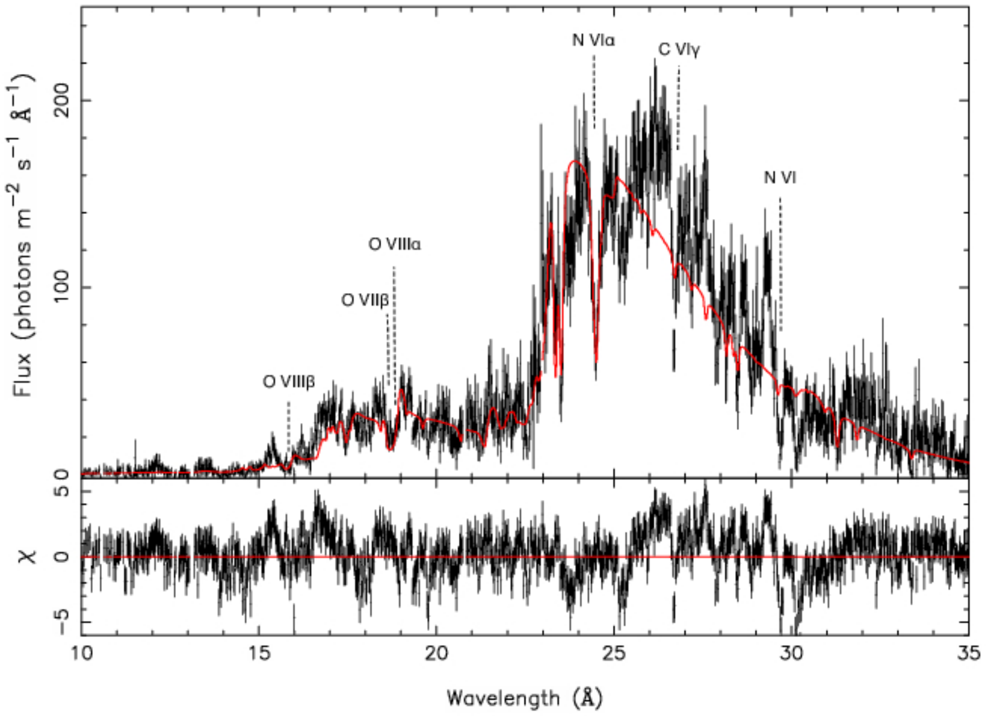

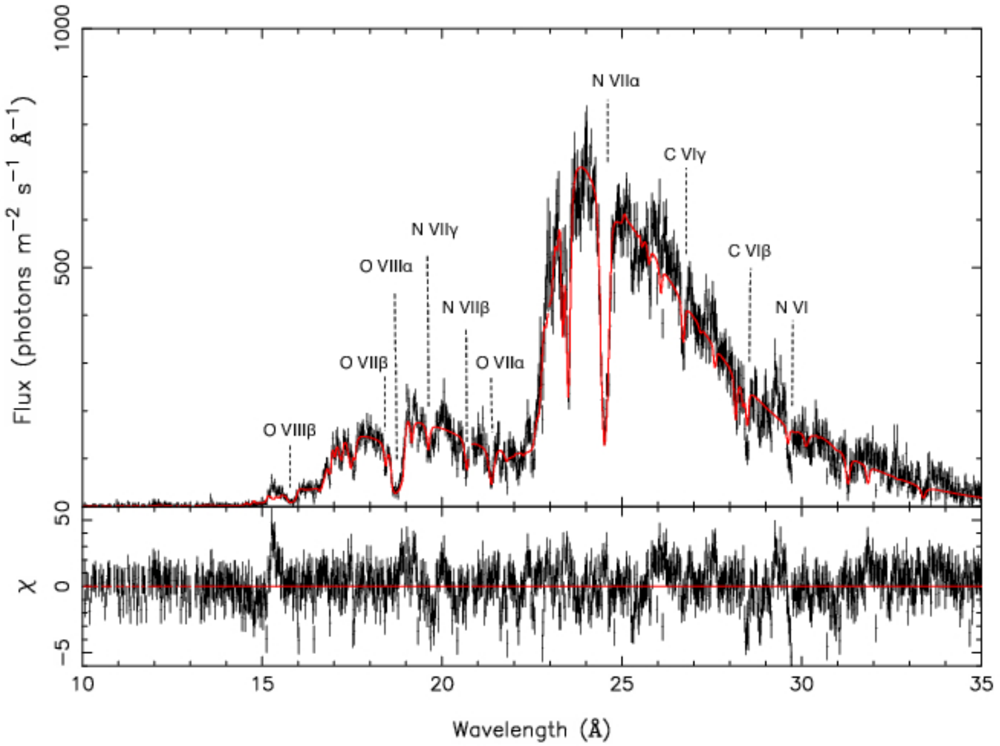

Region 2 (A2)

Region 3

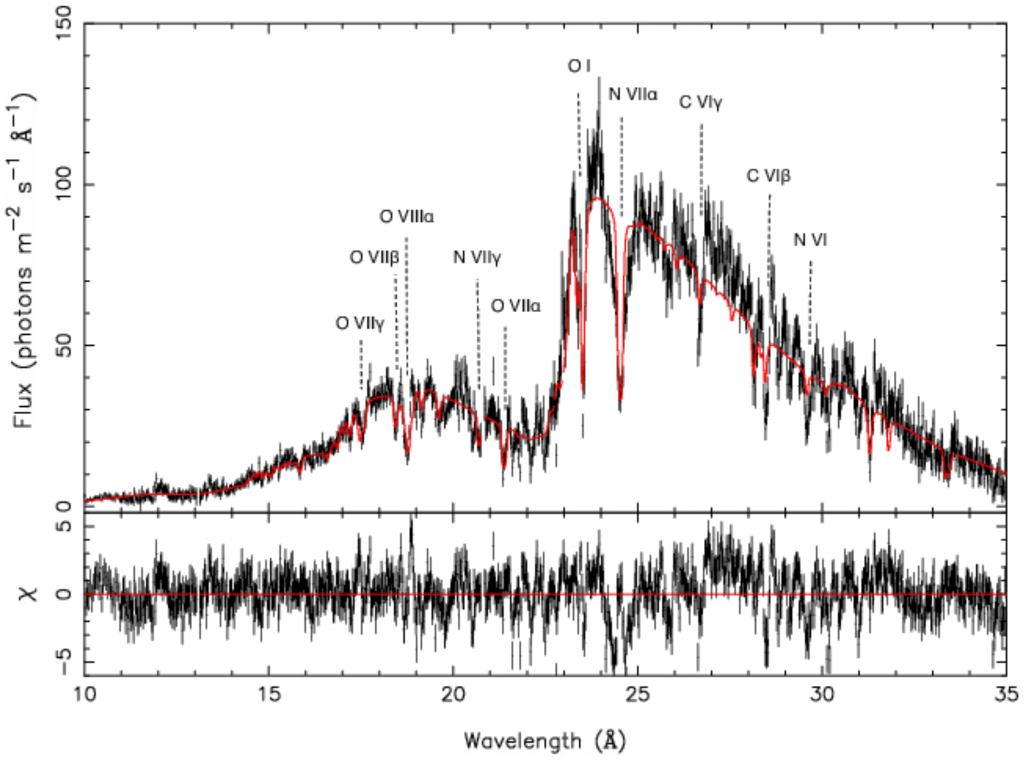

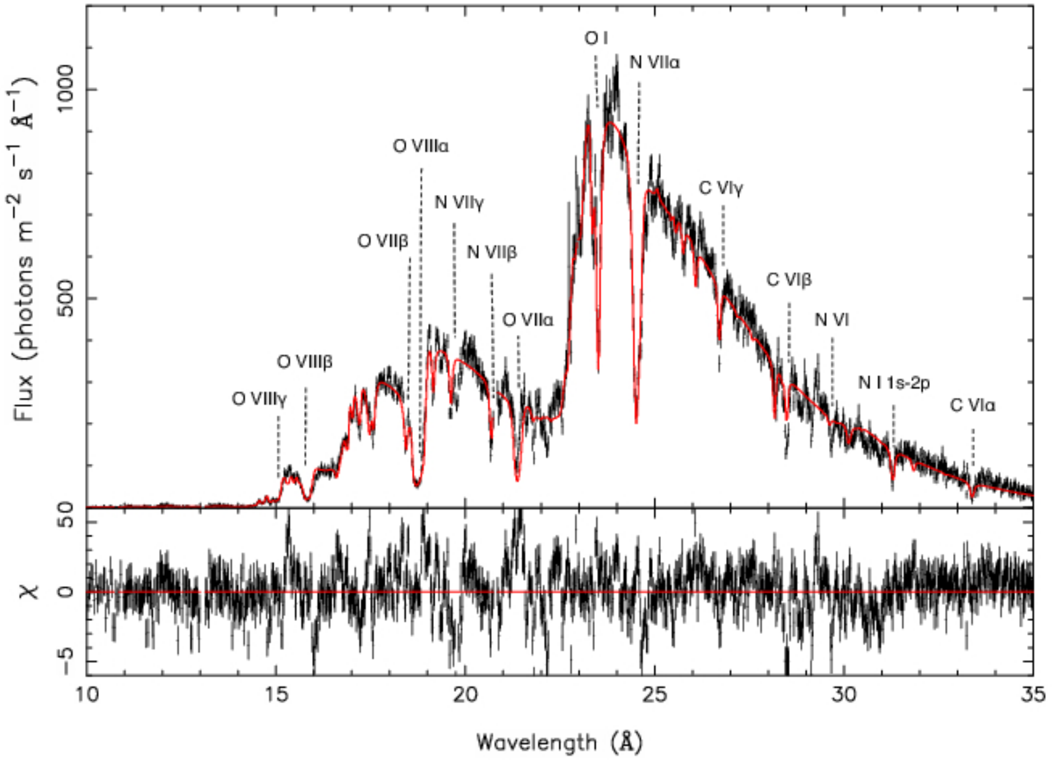

Second Obs. (Region B)

V2491 CYG SPECTRAL RESULTS

Model	Parameters	Region1	Region2	Region3	2nd Obs.
Blackbody	Norm (10^{20}cm^2)	$1.53^{+0.39}_{-0.25}$	$0.23^{+0.86}_{-0.04}$	$0.40^{+0.47}_{-0.21}$	$0.02^{+0.05}_{-0.01}$
	Temperature (eV)	$68.5^{+0.9}_{-0.9}$	$64.5^{+0.6}_{-3.6}$	$88.4^{+2.7}_{-1.8}$	$75.7^{+9.1}_{-6.5}$
	Luminosity(10^{39} erg s^{-1})	2.18	0.23	1.92	0.05
CIE	Norm (10^{58}cm^{-3})	$0.40^{+0.11}_{-0.09}$	$0.72^{+0.79}_{-0.32}$	$0.42^{+0.13}_{-0.05}$	$0.27^{+0.06}_{-0.1}$
	Temperature (keV)	$0.20^{+0.01}_{-0.01}$	$0.16^{+0.03}_{-0.02}$	$0.20^{+0.01}_{-0.01}$	$0.30^{+0.13}_{-0.03}$
	v_{mic} (km s^{-1})	2791	2791	2791^{+333}_{-288}	25068^{+1383}_{-951}
	Ne Abundance	2.45	2.45	$2.45^{+1.36}_{-0.92}$	$2.4^{+0.9}_{-0.9}$
	Mg Abundance	1.2	1.2	$1.2^{+1.0}_{-0.6}$	$1.98^{+0.70}_{-0.70}$
	Luminosity(10^{36} erg s^{-1})	1.31	1.78	1.38	0.77
HOT-1	N_H (10^{24}cm^{-2})	$0.40^{+0.03}_{-0.03}$	$0.09^{+0.03}_{-0.01}$	$0.07^{+0.01}_{-0.01}$	$0.19^{+0.10}_{-0.02}$
	Temperature (keV)	$2.63^{+0.96}_{-0.56}$	$1.77^{+0.17}_{-0.12}$	$1.06^{+0.03}_{-0.03}$	$1.38^{+0.38}_{-0.12}$
	σ_v rms velocity (km s^{-1})	872^{+25}_{-24}	827^{+61}_{-86}	879^{+12}_{-12}	114^{+18}_{-15}
	velocity shift (km s^{-1})	-3186^{+51}_{-50}	-3699^{+113}_{-173}	-3128^{+30}_{-31}	-2636^{+47}_{-45}
HOT-2	N_H (10^{24}cm^{-2})	$0.86^{+0.03}_{-0.03}$	$0.18^{+0.01}_{-0.02}$	$1.80^{+0.02}_{-0.02}$	$0.51^{+0.02}_{-0.05}$
	Temperature (keV)	$0.81^{+0.03}_{-0.03}$	$0.58^{+0.07}_{-0.11}$	$0.99^{+0.03}_{-0.03}$	$0.82^{+0.05}_{-0.45}$
	σ_v rms velocity (km s^{-1})	54^{+8}_{-9}	< 9	56^{+4}_{-5}	60^{+7}_{-8}
	velocity shift (km s^{-1})	-3180^{+71}_{-58}	-3038^{+6}_{-183}	-3194^{+30}_{-31}	-3550^{+36}_{-33}
Abundances	C Abundance	0.43	0.43	$0.43^{+0.07}_{-0.07}$	0.43
	N Abundance	5.2	5.9	$5.9^{+0.5}_{-0.9}$	5.9
	O Abundance	37.9	37.9	$37.9^{+3.8}_{-10.0}$	37.9
	Si Abundance	0.02	0.02	< 0.02	0.02
	S Abundance	0.02	0.02	$0.02^{+0.01}_{-0.01}$	0.02
	Ar Abundance	1.6	1.6	$1.6^{+3.9}_{-1.2}$	1.6
	Ca Abundance	0.01	0.01	< 0.01	0.01
	Fe Abundance	8.9	8.9	$8.9^{+3.8}_{-2.1}$	8.9
HOT-ISM	N_H (10^{21}cm^{-2})	$3.89^{+0.06}_{-0.06}$	$3.84^{+0.06}_{-0.19}$	$3.26^{+0.05}_{-0.09}$	$2.4^{+0.3}_{-0.2}$
	Temperature (eV)	$1.11^{+0.03}_{-0.04}$	$1.20^{+0.02}_{-0.04}$	$1.01^{+0.02}_{-0.02}$	$0.8^{+0.3}_{-0.3}$
	N Abundance	1.16	1.16	$1.16^{+0.12}_{-0.12}$	1.16
	O Abundance	1.75	1.75	$1.75^{+0.04}_{-0.02}$	1.75
	Fe Abundance	0.95	0.95	$0.95^{+0.13}_{-0.12}$	0.95
AMOL (Dust)	O_2 (10^{17}cm^{-2})	$0.34^{+0.13}_{-0.13}$	$2.3^{+0.2}_{-0.2}$	< 0.1	$1.3^{+0.1}_{-0.1}$
	H_2O(ice) (10^{17}cm^{-2})	$5.5^{+0.3}_{-0.3}$	$7.8^{+0.3}_{-0.5}$	$4.77^{+0.13}_{-0.13}$	$7.2^{+0.2}_{-0.2}$
	CO (10^{17}cm^{-2})	$1.28^{+0.13}_{-0.13}$	$0.27^{+0.2}_{-0.2}$	$0.1^{+0.07}_{-0.06}$	< 0.1
	χ^2_ν (d.o.f.)	1.80 (1415)	2.4 (1439)	2.86 (1440)	2.3 (1465)

Model	Parameters	Region1	Region2	Region3	2nd Obs.
Blackbody	Norm (10^{20}cm^2)	$0.99^{+0.06}_{-0.06}$	$0.46^{+0.05}_{-0.05}$	$0.40^{+0.01}_{-0.01}$	$0.02^{+0.01}_{-0.01}$
	Temperature (eV)	$68.1^{+0.5}_{-0.5}$	$63.1^{+1}_{-0.8}$	$84.6^{+0.4}_{-0.4}$	$79.9^{+1.2}_{-1.2}$
	Luminosity(10^{39} erg/s)	1.37	0.43	1.57	0.06
CIE	Norm (10^{58}cm^{-3})	$0.97^{+0.47}_{-0.37}$	$1.14^{+0.71}_{-0.40}$	$0.42^{+0.13}_{-0.05}$	$0.55^{+0.04}_{-0.04}$
	Temperature (keV)	$0.18^{+0.02}_{-0.01}$	$0.17^{+0.02}_{-0.02}$	$0.19^{+0.01}_{-0.01}$	$0.26^{+0.01}_{-0.01}$
	v_{mic} (km s^{-1})	2914	2914	2914^{+612}_{-510}	22410^{+1688}_{-1466}
	Ne Abundance	2.45	2.45	$2.45^{+1.36}_{-0.92}$	$2.4^{+0.9}_{-0.9}$
	Mg Abundance	1.2	1.2	$1.2^{+1.0}_{-0.6}$	$1.98^{+0.70}_{-0.70}$
	Luminosity(10^{36} erg s^{-1})	1.34	1.49	1.18	0.88
HOT-1	N_H (10^{24}cm^{-2})	$0.08^{+0.01}_{-0.01}$	$0.13^{+0.26}_{-0.05}$	$0.06^{+0.01}_{-0.01}$	$0.16^{+0.09}_{-0.02}$
	Temperature (keV)	$0.95^{+0.04}_{-0.04}$	$2.48^{+0.32}_{-0.35}$	$0.94^{+0.02}_{-0.02}$	$1.19^{+0.86}_{-0.20}$
	σ_v rms velocity (km s^{-1})	892^{+43}_{-41}	634^{+131}_{-156}	932^{+23}_{-23}	133^{+31}_{-28}
	velocity shift (km s^{-1})	-3304^{+83}_{-83}	-3805^{+229}_{-278}	-3250^{+51}_{-51}	-2826^{+88}_{-97}
HOT-2	N_H (10^{24}cm^{-2})	$0.76^{+0.02}_{-0.02}$	$0.44^{+0.05}_{-0.24}$	$1.61^{+0.01}_{-0.01}$	$0.71^{+0.01}_{-0.14}$
	Temperature (keV)	$0.89^{+0.05}_{-0.04}$	$0.59^{+0.02}_{-0.1}$	$1.06^{+0.02}_{-0.02}$	$0.68^{+0.01}_{-0.19}$
	σ_v rms velocity (km s^{-1})	< 37	< 20	35^{+14}_{-18}	< 17
	velocity shift (km s^{-1})	-3309^{+84}_{-103}	-3073^{+161}_{-191}	-3334^{+38}_{-36}	-3660^{+75}_{-65}
XABS	N_H (10^{20}cm^{-2})	$2.68^{+0.4}_{-0.3}$	$3.85^{+40}_{-2.56}$	$2.79^{+0.1}_{-0.1}$	$0.56^{+0.06}_{-0.06}$
	Log ξ (erg cm s^{-1})	$2.04^{+0.14}_{-0.16}$	$3.64^{+1.35}_{-0.2}$	$2.18^{+0.05}_{-0.05}$	$0.41^{+0.08}_{-0.07}$
	σ_v rms velocity (km s^{-1})	49^{+126}_{-18}	< 15831	53^{+10}_{-9}	195^{+78}_{-58}
	velocity shift (km s^{-1})	-3013^{+100}_{-368}	-1093^{+1294}_{-343}	-2968^{+47}_{-44}	-3127^{+127}_{-118}
Abundances	C Abundance	0.38	0.38	$0.38^{+0.07}_{-0.07}$	0.38
	N Abundance	5.8	5.8	$5.8^{+0.2}_{-0.2}$	5.8
	O Abundance	15.9	15.9	$15.9^{+0.5}_{-0.5}$	15.9
	Si Abundance	0.06	0.06	< 0.06	0.06
	S Abundance	0.02	0.02	$0.02^{+0.02}_{-0.01}$	0.02
	Ar Abundance	0.5	0.5	< 0.5	0.5
	Ca Abundance	0.02	0.02	< 0.02	0.02
	Fe Abundance	8.9	8.9	$8.9^{+3.8}_{-2.1}$	8.9
HOT-ISM	N_H (10^{21}cm^{-2})	$3.81^{+0.05}_{-0.05}$	$4.15^{+0.05}_{-0.06}$	$3.31^{+0.02}_{-0.02}$	$2.4^{+0.1}_{-0.1}$
	Temperature (eV)	$1.09^{+0.07}_{-0.3}$	$1.20^{+0.03}_{-0.05}$	$1.01^{+0.04}_{-0.04}$	$0.8^{+0.1}_{-0.1}$
	N Abundance	1.12	1.12	$1.12^{+0.13}_{-0.14}$	1.12
	O Abundance	1.68	1.68	$1.68^{+0.02}_{-0.02}$	1.68
	Fe Abundance	0.81	0.81	$0.81^{+0.13}_{-0.12}$	0.81
AMOL (Dust)	O_2 (10^{17}cm^{-2})	$0.47^{+0.61}_{-0.03}$	$1.48^{+0.23}_{-0.24}$	< 0.4	$0.9^{+0.1}_{-0.1}$
	H_2O(ice) (10^{17}cm^{-2})	$5.1^{+1.2}_{-0.1}$	$7.4^{+0.5}_{-0.5}$	$4.65^{+0.3}_{-0.7}$	$6.4^{+0.2}_{-0.2}$
	CO (10^{17}cm^{-2})	$1.34^{+0.53}_{-0.03}$	$0.29^{+0.2}_{-0.2}$	$0.16^{+0.07}_{-0.06}$	< 0.2
	χ^2_ν (d.o.f.)	1.73 (1411)	2.38 (1435)	2.46 (1436)	2.06 (1463)

THE HOT ABSORBERS AND THE WARM ABSORBER IN V2491 CYG

- **Two different hot absorber components** from our fits with blue shifts yielding **2850-3800 km s^{-1}** for the first (**day 40**) and **2600-3600 km s^{-1}** for the second observation **50 days** after outburst consistent with ejecta/wind speeds (Ness+2011) and HST-detected bipolar and equatorial outflows (Riberio+2011).
- The two collisionally ionized hot absorption (in equilibrium) components have temperatures **$kT_1 \simeq 1.0 – 3.6$ keV** and **$kT_2 \simeq 0.4 – 0.87$ keV** with rms **velocities $\sigma_{v1} \simeq (740 – 900)$ km/s** and **$\sigma_{v2} \simeq (9 – 67)$ km/s**. → Consistent with shock temperatures in the X-ray wavelengths for the given days after outburst → 1.0-4.0 keV (see Page+ 2010).
- The equivalent hydrogen column density of the hot collisionally ionized absorbers are $(0.6\text{-}18.0)\times10^{23}$ cm^{-2} and $(2.0\text{-}5.3)\times10^{23}$ cm^{-2} on days 40 and 50 after outburst.
- **An additional photoionized absorber** (third intrinsic absorber component) in the shell/ejecta improves the fits, but shows only (1-0.1)% of the absorption by the collisionaly-ionized hot gas (**$\sigma_v \simeq (31 – 170)$ km/s day 40** and **$(140 – 275)$ km/s day 50.** The column density is **$(1.3\text{-}4.3)\times10^{20}$ cm^{-2} and $(0.5\text{-}0.7)\times10^{20}$ cm^{-2}** on days 40 and 50.

THE WD, USING SPECTRAL RESULTS

- Our blackbody temperatures are in a range 61-91 eV ((8.3-10.0)$\times 10^5$ K), slightly variable over the two observations) with 62-85 eV from the best fit value range (Table 2).
- The temperature ranges obtained using the fits with photoionized absorbers are 81-123 eV for day 40 and 94-96 eV (9.6-10.5$\times 10^5$ K) for day 50 (Pinto+ 2012)
- White dwarf (WD) mass is 1.15-1.3 $M_\odot$ **assuming our range** is the maximum temperature achieved during the H-burning phase. WD radius → (27-30)$\times 10^8$ cm for the region 1; (17-20)$\times 10^8$ cm for the regions 2, 3 on day 40 and (2.8-4.9)$\times 10^8$ cm on day 50. A C-O WD (4.5-2.8)$\times 10^8$ cm for 1.15-1.3 $M_\odot$ (Hamada & Salpeter 1961; Panei+ 2000).
- V2491 Cyg shows signature of H-burning with underabundant carbon from our fits $C/C_\odot$ =0.3-0.5, and enhanced nitrogen $N/N_\odot$ =5-7 and oxygen $O/O_\odot$ =16-43 ($Ne/Ne_\odot$ =1.3-3.8).
- Munari+ 2011 (ground-based optical obs) found $Fe/Fe_\odot$ = 0.6, $O/O_\odot$ = 4.3, $N/N_\odot$ =59, and $Ne/Ne_\odot$ =6.5. van Rossum & Ness (2010) have only assumed solar abundances for simplicity and Ness+ 2011 have found consistent fits using static NLTE atmosphere models with fixed abundances where oxygen abundance was in a range $O/O_\odot$ = 10-30.

Preliminary Analysis on V4743 Sgr

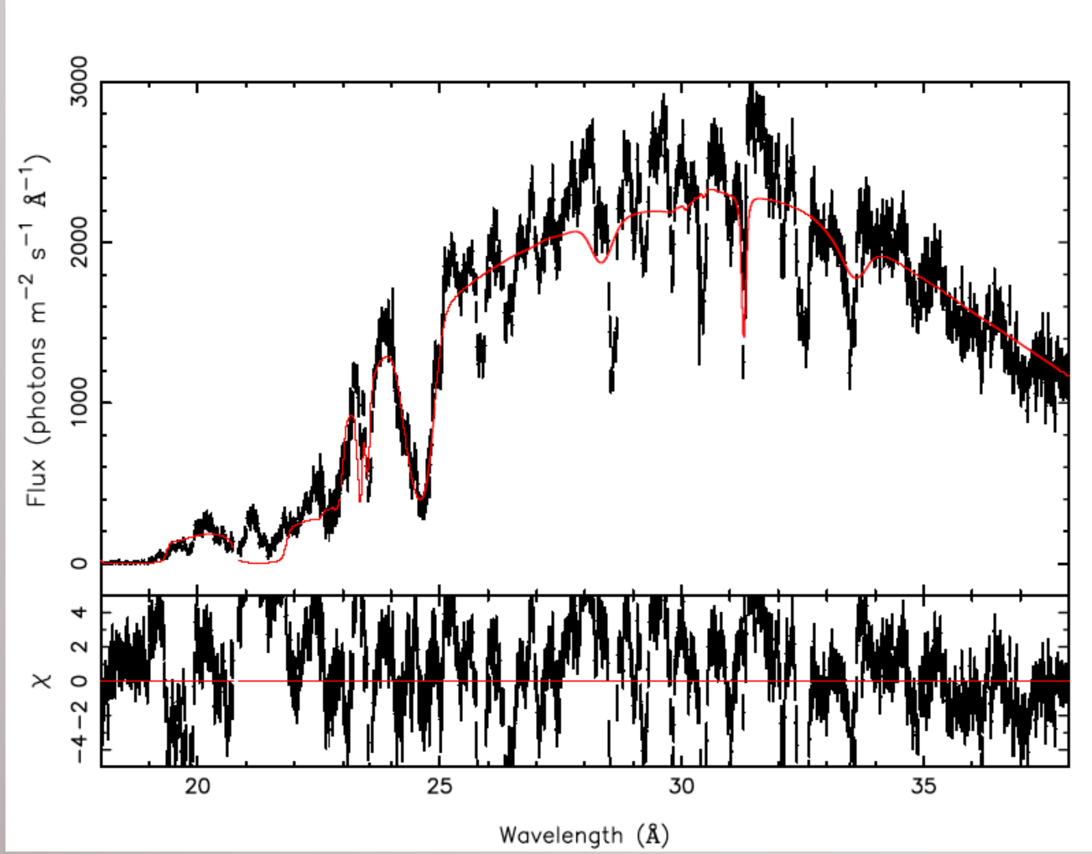

(Gamsızkan & Balman in preperation, 2017)

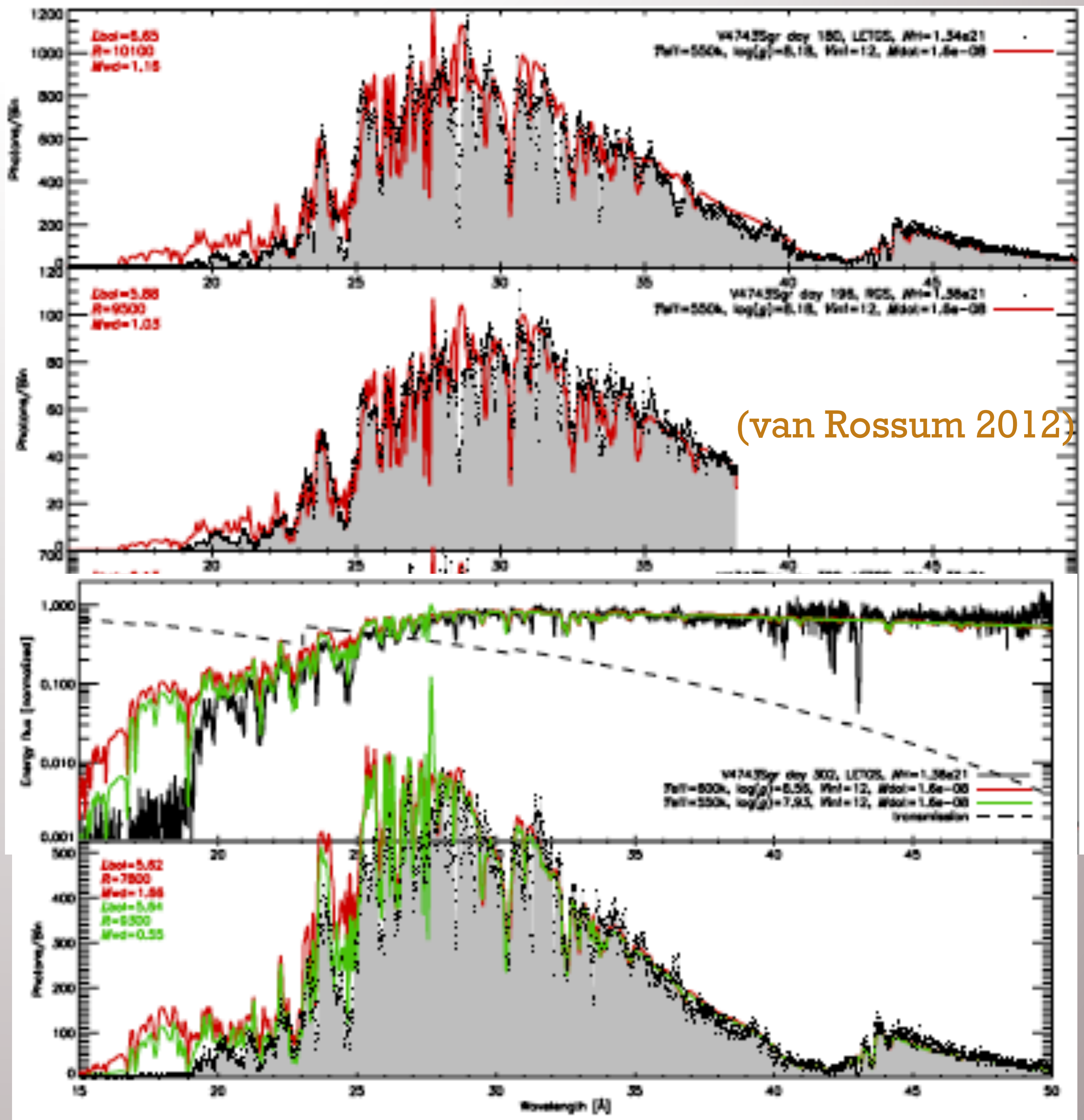

(van Rossum 2012)

Includes one Hot and one Xabs model
BB temp. 47 eV, ionization parameter 2.88,
Hot absorber temperature 3.5 keV
CNO – carbon depleted, N and C enhanced
over factor 10 w.r.t. solar abund. χ^2_ν = 10(1149)

FUTURE PROSPECTS

- ✓The X-ray absorption in classical/ recurrent novae spectra during the outburst stage is complicated → **photospheric** + **warm photoionized** absorption + **hot collisionally ionized** absorption originating from a nova wind/ ejecta + the **interstellar absorption from gas and dust (may be intrinsic)** in the line of sight.

- ✓Our work on the XMM-Newton RGS data of V2491 Cyg yields **two main hot collisionally ionized (in equilibrium) absorber** components with different temperatures, rms velocities and equivalent column densities originating in the shocked fast moving ejecta/wind → high and low density regions with different turbulent conditions and temperatures in the ejecta/wind indicating the inhomogeneity (e.g., oxygen-dense regions) and mixed morphology of the outflow.

- ✓We plan to extend our analysis to other existing data on novae and possible super soft X-ray sources to study how complex absorption affects X-ray spectra and how the stellar continuum is shaped during the course of the outburst evolution. We also aim to utilize plausible different continuum models as in stellar atmosphere models.